Acoustic Bloch oscillations in a two-dimensional phononic crystal

Zhaojian He, Shasha Peng, Feiyan Cai, Manzhu Ke, and Zhengyou Liu*
Key Lab of Acoustic and Photonic Materials and Devices of Ministry of Education and Department of Physics, Wuhan University, Wuhan 430072, China

(Received 8 June 2007; revised manuscript received 13 September 2007; published 12 November 2007)

We report the observation of acoustic Bloch oscillations at megahertz frequency in a two-dimensional phononic crystal. By creating periodically arrayed cavities with a decreasing gradient in width along one direction in the phononic crystal, acoustic Wannier-Stark ladders are created in the frequency domain. The oscillatory motion of an incident Gaussian pulse inside the sample is demonstrated by both simulation and experiment.

DOI: 10.1103/PhysRevE.76.056605 PACS number(s): 46.40.Cd, 43.20.+g, 43.40.+s

An electron in a periodic potential (a crystal) subjected to an external field is first accelerated and then slowed down until it reaches the top of the energy band or the Brillouin zone boundary, where it reverses direction. In real space, the electron keeps moving back and forth, oscillating in a localized area. This phenomenon is well known as (electronic) Bloch oscillations (EBOs), and the corresponding electronic states are the Wannier-Stark ladder (WSL) states [1,2]. But an electron in a crystal always experiences scattering from the imperfections of the crystal, and even Zener tunneling when an external field is applied, and these dephasing effects usually have a characteristic time shorter than the oscillatory period h/eFd, where e is the electronic charge, F is the applied electric field, and d is the lattice constant. Therefore it is not easy to observe EBOs in a conventional crystal. Until now, EBOs have been observed only in semiconductor superlattices [3,4], thanks to the bigger lattice constant d of superlattices, which results in an oscillatory period smaller than the dephasing time. Recently, there is growing interest in Bloch oscillations for photons in photonic crystals or phonons in phononic crystals [5–7]. Because an electric field has no effect on photons and phonons, different methods are used to incline the photonic or phononic bands in these investigations. The typical method is to introduce periodic cavities along one direction in the photonic or phononic crystal by allowing the cavities to have a gradient in cavity width or in the refractive index of the cavity material. Optical Bloch oscillations have been realized both in theory and in experiment in one-dimensional optical superlattices with cavities of refractive index gradient along the growth direction [5,6]. Phonon Bloch oscillation and Raman spectra of phononic WSL states have been described in nanosized multilayer structures based on phonon cavities of increasing thickness [7]; on a larger scale, WSLs and Bloch oscillations for elastic or acoustic waves have also been demonstrated in one-dimensional structures [8,9]. In addition, it was predicted that acoustic Bloch oscillations (ABOs) should be observed in two-dimensional phononic crystals made of rigid cylinders in water [10].

*Author to whom all correspondence should be addressed. zyliu@whu.edu.cn

In this paper, we demonstrate that acoustic Bloch oscillations can be truly realized in two-dimensional phononic crystals made of steel cylinders in water. By introducing periodical arrayed cavities into the phononic crystal, and allowing the cavities to have a gradient in width along the translating direction, minibands are created in the band gap of the phononic crystal and inclined along this direction. Both the theoretical and experimental transmission spectra of the structure show clearly the feature of acoustic WSLs, indicating that it was possible for ABOs to be established inside the phononic crystal. Time-resolved ABOs are demonstrated by numerical simulations based on the multiple-scattering theory (MST), and confirmed by the agreement of the calculation and the measurement for time-resolved transmission spectra. This is also a demonstration of ABOs in phononic crystals with dimension higher than 1.

The phononic crystal we use consists of a square array of steel cylinders in water, with four cavities created along the Γ-X direction (z direction) as schematically shown in Fig. 1(a). The lattice constant of the base phononic crystal is $a=1.7$ mm and the radius of the steel cylinders is $R=0.5$ mm. Without the cavities, the (base) phononic crystal has a band structure as shown in Fig. 1(b), calculated with the MST method [11]. A band gap extending from 0.34 to 0.52 MHz can be clearly seen along the Γ-X direction. With the cavities (of width $2a$), the superlattice in Fig. 1(a) has a band structure as shown in Fig. 1(c). Since the translation period ($5a$) of the superlattice is five times bigger than the original phononic crystal along this direction; the Brillouin zone of the superlattice along this direction is five times smaller. We observe that there are two minibands in the original gap region, with frequency ranging from 0.36 to 0.39 MHz and from 0.48 to 0.51 MHz, respectively, which are the result of the coupling of cavity modes [12–17]. The coupling of cavity modes supplies a passage to the acoustic waves; as a result, mini pass bands emerge. These minibands are essential for realizing ABOs, because they may easily be inclined along the cavities' translation direction by tuning the properties of the cavities. The simplest way to incline the minibands is to supply a width gradient to the cavities along the translation direction. For this purpose, beginning from cavity W_1 [see Fig. 1(a)], we gradually reduce the cavity width d_i ($i=1,2,3$) with a decrement $\delta=0.12a$. In this way, the four cavities from W_0 to W_3 would

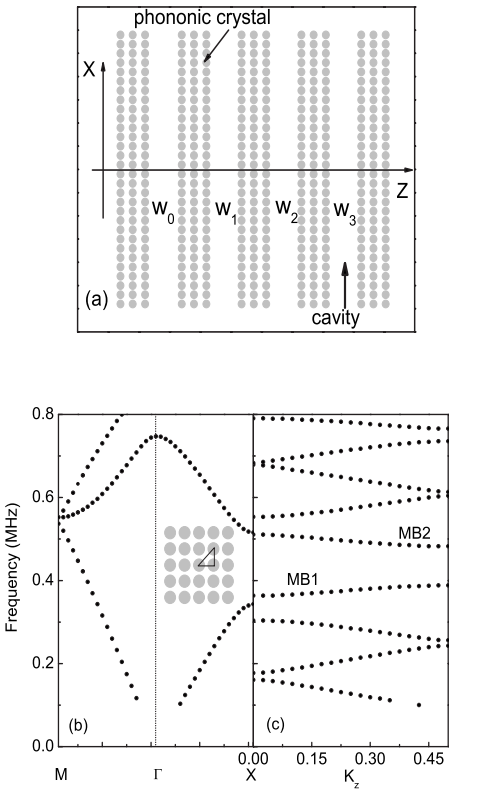

FIG. 1. (a) Two-dimensional phononic crystal with four cavities, designed to demonstrate ABOs; the base phononic crystal consisting of a square array of steel cylinders in water. (b) Band structure of the base phononic crystal without the cavities. (c) Band structure along the z direction for the superlattice shown in (a), the cavities having a width of $d=2a$; two minibands denoted by MB1 and MB2 are induced by the cavities in the Γ-X directional gap. k_z is in units of $\pi/5a$.

have a new width d_i $(i=0,1,2,3)$ being $2a$, $1.88a$, $1.76a$, and $1.64a$ in sequence. Since the minibands come from the coupling of the cavity modes, the central frequency of the minibands is thus governed by the cavity modes, which have frequencies approximately inversely proportional to the cavity width. Hence the central frequency of the minibands can be written down as $f \propto 1/d$, where d is the cavity width. The decrease of the cavity widths along the z direction means an increase of the central frequency of the minibands, i.e., $f_i \propto 1/d_i = 1/(d_0 - i\delta)$, so that the minibands are inclined up along this direction. Therefore, the inclination of the minibands in this way is generally not linear with the position along the z direction, unless the decrement δ is very small. When δ is very small, $\Delta f = f_{i+1} - f_i \propto 1/\delta$ is uniform along the z direction, such that for each infinite periodic structure with cavities of a given width d_i $(i=0,1,2,3)$, the two minibands have frequency ranges. The inclination of the two minibands along the z direction for this sample is given in Fig. 2(a), similar to the cases in photonic crystals [5,6]. With the sample prepared, we measure the transmission spectra based on the well-known ultrasonic transmission technique [18,19]. In the experiment, the sample is placed between a generating transducer and a detecting transducer, and the entire assembly is immersed in a water tank. A pulser-receiver generator (Panametrics model 5800PR) produces a short-duration pulse. The generating transducer is placed far away from the sample to yield an input pulse approximating a plane wave. The input pulse is determined by measuring its amplitude and phase in water without the sample in place. The pulses transmitted through the sample are detected by an immersion transducer. Both the generating transducer and the detective transducer have the central frequency of 0.5 MHz and the diameter of 25.4 mm. In Fig. 2(b), we show the measured transmission spectra with open circles. In order to compare with theory, we also show in this figure the calculated transmission spectra obtained with the MST method [20] as denoted with solid circles. The pass bands and band gaps can be clearly identified in the spectra, and the theory and the experiment show an overall agreement. The magnitude discrepancy of the transmissions in theory and experiment mainly comes from the absorption existing in the system. Since several cavities are involved, the cavity mode resonances (which are just the cause of the minibands) make absorption more remarkable. In spite of the discrepancy in the magnitude of the transmission coefficients, the most important features relevant to the ABOs are well preserved in both the calculated and measured transmission spectra, which are the oscillations in the spectral region corresponding to two tilted minibands. Each peak in each miniband corresponds to a single WSL state, which is the frequency domain counterpart of a time-resolved ABO. Therefore, it is expected that within the frequency of the minibands, it should be possible to observe ABOs in the time domain.

To demonstrate the ABOs in the time domain, we launch a Gaussian pulse into the sample. The Gaussian pulse is described by $g(f)=\exp\{-4\pi[(f-f_0)/\sigma]^2\}$, with the central frequency $f_0=0.52$ MHz located in the upper miniband, and $\sigma=0.05$ MHz. In response to the incident pulse, the time and spatial variations of the displacement field $u(z,t)$ inside the sample can be calculated according to the scattering state method as [21]

$$u(z,t) = 1/2\pi \int_{-\infty}^{\infty} u(z,f)g(f)\exp(-i2\pi ft)df, \qquad (1)$$

where $u(z,f)$ is the displacement field distribution for each frequency, which can be obtained by the MST method. Figure 3 shows the simulation result, where the oscillatory motion of the pulse is clearly observed in real time. We see that at $t=0$ the pulse enters the structure at the surface $z=0$, then tunnels through the forbidden band, and finally starts to oscillate within the inclined miniband inside the sample with a regular period. The period can roughly be estimated as 70 μs.

Since it is difficult to measure the field distribution inside the sample (the say nothing of the temporal field distribution), it is hard to experimentally demonstrate an ABO in the same way as in the simulation. Since the ABO inside the sample affects the time-resolved transmission or reflection spectra, the ABO can be alternatively demonstrated by measuring the time-resolved transmission or reflection spectra. According to the scattering state method, the time-resolved transmission coefficients can be calculated from

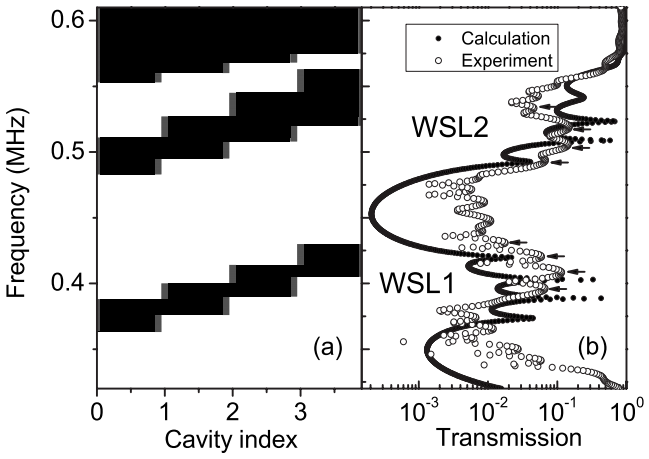

FIG. 2. (a) Two minibands (dark regions) across the sample, tilted by the gradient of the cavity width. White regions stand for gaps. (b) Corresponding calculated (solid circles) and measured (open circles) transmission spectra of the sample. The peaks in the frequency region of each miniband can be clearly seen, which correspond to the WSLs. The arrows indicate the experimental peaks.

$$T(t) = 1/2\pi \int_{-\infty}^{\infty} T(f)g(f)\exp(-i2\pi ft)df, \qquad (2)$$

where $T(f)$ is the transmission coefficient for frequency f, which can be obtained by the MST method. To measure the time-resolved transmission spectrum corresponding to the simulated ABO, a pair of plane transducers is used as described in the transmission measurement, which has a central frequency of 0.5 MHz and a frequency width of about 0.3 MHz. The incident pulse signal of the transducer is shown in the inset of Fig. 4(a). By measuring the time-resolved transmission spectrum of the whole pulse and filtering it to a frequency window that just covers four Wannier-Stark states in the corresponding upper miniband, we obtain

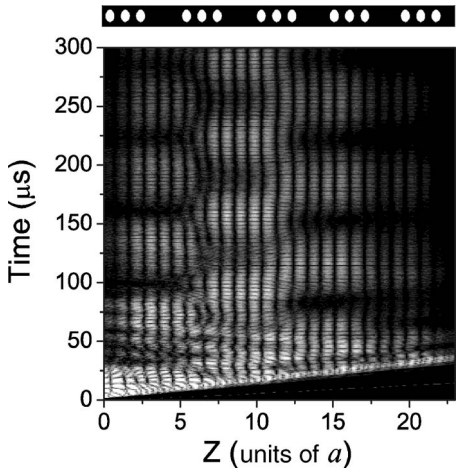

FIG. 3. Field distribution across the sample along the z axis [see Fig. 1(a)] varying with time, for reference, the sample is schematically drawn on the top. A change from dark to bright corresponds to an increase of intensity. The ABO in the time domain is clearly seen.

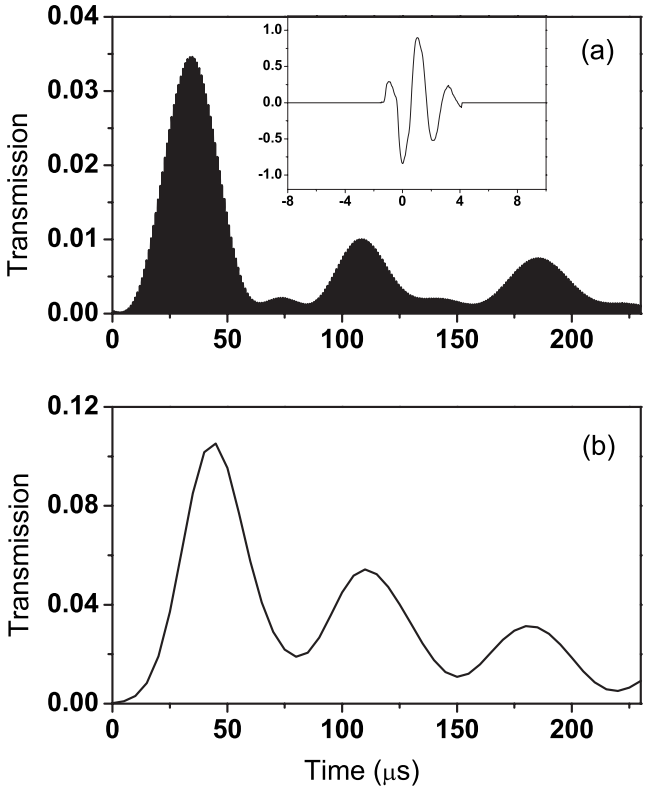

FIG. 4. Time-resolved transmission spectra of the sample in arbitrary units, showing three oscillating cycles, the oscillation period of the ABO is 70 μs. (a) Experiment and (b) calculation. The incident pulse signal of the transducer is shown in the inset of (a).

the desired time-resolved transmission spectrum as shown in Fig. 4(a). Within the time range of the measurement, three oscillatory cycles are clearly observed. For comparison, we show in Fig. 4(b) the calculated time-resolved transmission coefficient with a Gaussian incident pulse. We see that there is a rather good agreement between the simulation and the experiment. An oscillating period of 70 μs for the ABO can be obtained from the two time-resolved spectra, in agreement with the rough estimation from the real time simulation above.

In conclusion, we investigated acoustic Bloch oscillations in a two-dimensional phononic crystal. By creating periodically arrayed cavities with decreasing gradient in width along one direction in the phononic crystal, acoustic Wannier-Stark ladders were established in the structure. The numerical simulation clearly shows acoustic Bloch oscillation inside the sample when a Gaussian pulse with central frequency close to the Wannier-Stark ladders is incident into the sample. The measured time-resolved transmission spectrum has good agreement with the calculation; both show the acoustic Bloch oscillation having a period of 70 μs.

ACKNOWLEDGMENT

This work is supported by the National Natural Science Foundation of China (Grant No. 50425206, No. 10731160613, and No. 50702038).

[1] F. Bloch, Z. Phys. **52**, 555 (1928); C. Zener, Proc. R. Soc. London, Ser. A **145**, 523 (1934).
[2] H. M. James, Phys. Rev. **76**, 1611 (1949); G. H. Wannier, *ibid.* **100**, 1227 (1955).
[3] J. Feldmann, K. Leo, J. Shah, D. A. B. Miller, J. E. Cunningham, T. Meier, G. von Plessen, A. Schulze, P. Thomas, and S. Schmitt-Rink, Phys. Rev. B **46**, 7252 (1992).
[4] C. Waschke, Hartmut G. Roskos, Ralf Schweddler, Karl Leo, Hinrich Kurz, and Klaus Köhler, Phys. Rev. Lett. **70**, 3319 (1993).
[5] V. Agarwal, J. A. del Rio, G. Malpuech, M. Zamfirescu, A. Kavokin, D. Coquillat, D. Scalbert, M. Vladimirova, and B. Gil, Phys. Rev. Lett. **92**, 097401 (2004).
[6] Riccardo Sapienza, Paola Costantino, Diederik Wiersma, Mher Ghulinyan, Claudio J. Oton, and Lorenzo Pavesi, Phys. Rev. Lett. **91**, 263902 (2003).
[7] N. D. Lanzillotti Kimura, A. Fainstein, and B. Jusserand, Phys. Rev. B **71**, 041305(R) (2005); N. D. Lanzillotti Kimura, A. Fainstein, C. A. Balseiro, and B. Jusserand, *ibid.* **75**, 024301 (2007).
[8] L. Gutierrez, A. Díaz-de-Anda, J. Flores, R. A. Méndez-Sánchez, G. Monsivais, and A. Morales, Phys. Rev. Lett. **97**, 114301 (2006).
[9] Helios Sanchis-Alepuz, Yuriy A. Kosevich, and Jose Sanchez-Dehesa, Phys. Rev. Lett. **98**, 134301 (2007).
[10] Jose Sanchez-Dehesa, Helios Sanchis-Alepuz, Yuriy A. Kosevich, and Daniel Torrent, J. Acoust. Soc. Am. **120**, 3283 (2006).
[11] J. Mei, Z. Liu, J. Shi, and D. Tian, Phys. Rev. B **67**, 245107 (2003).
[12] M. Trigo, A. Bruchhausen, A. Fainstein, B. Jusserand, and V. Thierry-Mieg, Phys. Rev. Lett. **89**, 227402 (2002).
[13] A. Khelif, A. Choujaa, B. Djafari-Rouhani, M. Wilm, S. Ballandras, and V. Laude, Phys. Rev. B **68**, 214301 (2003).
[14] A. Khelif, B. Djafari-Rouhani, J. O. Vasseur, and P. A. Deymier, Phys. Rev. B **68**, 024302 (2003).
[15] S. X. Yang, J. H. Page, Z. Y. Liu, M. L. Cowan, C. T. Chan, and P. Sheng, Phys. Rev. Lett. **88**, 104301 (2002).
[16] C. Y. Qiu, Z. Y. Liu, J. Mei, and J. Shi, Appl. Phys. Lett. **87**, 104101 (2005).
[17] D. Feng and G. J. Jin, *Condensed Matter Physics* (Higher Education Press, Beijing, 2006), Vol. 1.
[18] S. X. Yang, J. H. Page, Z. Y. Liu, M. L. Cowan, C. T. Chan, and P. Sheng, Phys. Rev. Lett. **93**, 024301 (2004).
[19] F. R. Montero de Espinosa, E. Jiménez, and M. Torres, Phys. Rev. Lett. **80**, 1208 (1998).
[20] C. Y. Qiu, Z. Y. Liu, J. Mei, and J. Shi, Solid State Commun. **134**, 765 (2005).
[21] G. Malpuech and A. Kavoin, Semicond. Sci. Technol. **16**, R1 (2001).